Intercalation of Primary Diamines in the Layered Perovskite Oxides, $HSr_2Nb_3O_{10}$

Young-Sik Hong and Si-Joong Kim

Department of Chemistry, College of Science, Korea University, Seoul 136-701, Korea
Received April 26, 1996

The layered perovskite oxide, $KSr_2Nb_3O_{10}$, was synthesized. The interlayer potassium cations were readily exchanged by protons in hydrochloric acid solution to give the protonation compound, $HSr_2Nb_3O_{10}\cdot 0.5H_2O$. The intercalation compounds, $[NH_3(CH_2)_nNH_3]_xSr_2Nb_3O_{10}$, were also obtained by acid-base reactions between the protonation compound and organic bases, 1,n-alkyldiamines. The interlayer distances in the intercalation compounds were linearly increased with the increase of the number of carbon ($\Delta c/\Delta n = 1.05$ Å) in 1,n-alkyldiamines. The intercalated alkyldiammonium ions formed a paraffin-like monolayer with average tilting angle (θ) of *ca.* 56°. The intercalation reactions occurred stoichiometrically. The thermal decomposition process of the intercalation compounds showed distinct three steps due to the desorption of hydrated water, the decomposition of organic moiety, and the decomposition of Sr-related compounds.

Introduction

A number of layered oxides have been known which are made up of layers of corner-shared octahedra separated by large alkali metal cations.[1~2] Especially, two series of layered oxide phases based on the perovskite structure have been attracted due to their interesting physical properties. One is the Ruddlesden-Popper series having the general formula of $M_2[A_{n-1}B_nO_{3n+1}]$. Among them, Sr_2TiO_4, Sr_3TiO_7, and $Sr_4Ti_3O_{10}$ are well-known.[3] Two of the Sr atoms in each compound occupy nine coordinate sites between the perovskite $[Sr_{n-1}Ti_nO_{3n+1}]^{-2}$ layers. The layers are formed by limiting the extension of these lattices along one of the three cubic directions. The phases of these general types contain two metal cations per formula unit and show no interesting interlayer reaction chemistry because of the higher layer charge.

In 1981, the other layered perovskite oxides $MCa_2Nb_3O_{10}$ (M=K, Rb, Cs), possessing only a half of the cations in comparison to those of Ruddlesden-Popper oxides, were reported by Dion *et al.*.[4] As a consequence of this lower layer charge density, ion exchange of the interlayer monovalent cation can occur in acidic solution or molten salts to give ion-exchanged derivatives. The difference in reactivity for ion exchange reaction between Ruddlesden-Popper series and Dion series has an analogy in the 2 : 1 clay minerals.

Subsequently, Jacobson et al. have prepared $n=3$-7 members of the series with the general formula $K[Ca_2Na_{n-3}Nb_nO_{3n+1}]$ and Gopalakrishnan *et al.* have prepared the series of $n=2$ members in $M[A_{n-1}B_nO_{3n+1}]$.[5~6] Recently, several researchers reported on the synthesis and characterization of other related compounds such as $KLnNb_2O_7$, $A_2Ln_2Ti_3O_{10}$, $ABiNb_2O_7$ and $APbNb_2O_7$.[6~8]

The protonation compounds of these oxides, $H[A_{n-1}B_nO_{3n+1}]$, act as solid Brφnsted acids and react with organic bases to form intercalation compounds with larger basal expansions. In addition, the protonation compounds have attracted in view of potential application as solid acid catalysts and proton conductors.[9~10] It has also been shown that such intercalation compounds can be exfoliated into single layer and can be stuffed with polyhydroxyaluminate species at the interlayer spacing, yielding novel molecular composite.[11~12]

However, $KSr_2Nb_3O_{10}$, which is one of the simplest derivatives of $KCa_2Nb_3O_{10}$ has not been studied. In the present study, we synthesized the layered compound of $KSr_2Nb_3O_{10}$ and carried out protonation and intercalation reaction with alkyldiamines. The thermal stability of the intercalation compounds were also investigated.

Experimental

$KSr_2Nb_3O_{10}$ was synthesized by the calcination of the mixtures of K_2CO_3, $SrCO_3$, and Nb_2O_5 in air at 1150 ℃ for 2 days with a grinding in between.[4~5] A 25 mol% excess K_2CO_3 was added to compensate for the loss due to volatilization. The $KSr_2Nb_3O_{10}$ (12.06 g), was stirred in 6 N HCl (200 mL) solution at 60 ℃ and the exchange reaction was continued by renewing the acid solution every one day. The exchange was found to be complete in 4 days. Then the product was washed with deionized water, centrifuged, and dried in a vacuum oven. The intercalation reactions were performed with a 20% amine solution in water for $n=2$-8 and *n*-heptane for $n=10$ and 12 at 60-90 ℃ for 3 days.

The chemical analyses of $KSr_2Nb_3O_{10}$ and protonation compound were carried out by Energy-dispersive X-ray emission (EDX, JEOL JSM 840 A) method. The structures of the layered compounds were characterized by X-ray powder diffraction (XRD, Rigaku D-MAX III-b) and infrared spectroscopy (FT-IR, BOMEN MB-102).

In order to investigate the stacking sequence of intercalated organic molecules, one-dimensional electron density along c-axis, ρ(z), has been calculated from the Fourier transform of the structural factors, F_{00l}. For 1-D Fourier synthesis, the diffraction data were taken θ-2θ step scan procedure using the step 0.05° size and 5 sec per step. The contents of the interlayered water in protonation compound and the intercalated amine in the intercalation compounds were determined from weight losses in thermogravimetric analysis (TGA, STANTON REDCROFT TGA-1000) and elementary analysis (EA, CARLO ERBA, EA 1108).

Results and Discussion

Synthesis and proton exchange reaction of $KSr_2Nb_3O_{10}$. Powder XRD patterns of $KSr_2Nb_3O_{10}$ and protonation compound showed the formation of layered perovskite compounds analogous to the corresponding $KCa_2Nb_3O_{10}$ and $HCa_2Nb_3O_{10}\cdot 1.5H_2O$ phase already reported in the literature.[4] All the reflections could be indexed by using an orthorhombic cell in which c axis is perpendicular to the layers. The indexed powder diffraction data and the refined cell parameters are listed in Table 1 and Table 2, respectively. The crystal structure of $KSr_2Nb_3O_{10}$ was similar to that of $KCa_2Nb_3O_{10}$ phase which contains two perovskite layers displaced relative to each other by a/2.[5,13] The translation of adjacent layers results in trigonal-prismatic coordination for the interlayer potassium atoms. Unlike the $KSr_2Nb_3O_{10}$, the protonation compound showed no c-axis doubling. In the protonation compound, the layers are thus stacked to give an eight-coordinate interlayer site, whereas in potassium compound are displaced by half a unit cell to give a six-coordinate interlayer site because adjacent layers are stacked to optimize the coordination of the interlayer cations.

Chemical analysis by EDX showed that the atomic ratios of K : Sr : Nb are varied as expected from the formula of $KSr_2Nb_3O_{10}$ and protonation compound ($HSr_2Nb_3O_{10}$) within the instrumental error. The percentages of K, Sr, and Nb atoms in $KSr_2Nb_3O_{10}$ were 5.8 (6.0), 28.5 (26.8), and 40.7 (42.7) and protonation compound were 0.2 (0), 28.1 (28.5), and 46.2 (45.3), where numbers in the blanks denote calculated values, respectively. From the EDX analysis of the protonation compound, it was found that potassium ions in interlayer position were almost exchanged by protons. The Sr : Nb ratios were not altered and, from this, we deduced that Sr and Nb atom were not dissolved in HCl solution during the protonation reaction.

Table 1. Powder X-ray diffraction data for $KSr_2Nb_3O_{10}$ and $HSr_2Nb_3O_{10}\cdot 0.5H_2O$

$KSr_2Nb_3O_{10}$				$HSr_2Nb_3O_{10}\cdot 0.5H_2O$				
h k l	$d_{obs.}$(Å)	$d_{cal.}$(Å)	$I_{obs.}$	h k l	$d_{obs.}$(Å)	$d_{calc.}$(Å)	$I_{obs.}$
0 0 2	15.121	15.028	100	0 0 1	16.477	16.424	100
0 0 4	7.536	7.514	29	0 0 2	8.222	8.212	17
0 0 6	5.024	5.010	11	0 0 4	4.105	4.106	12
0 1 0	3.913	3.907	14	1 0 0	3.907	3.903	5
0 0 8	3.759	3.757	15	1 0 2	3.526	3.525	3
1 0 3	3.655	3.651	10	0 0 5	3.282	3.285	3
1 0 5	3.283	3.284	12	1 0 3	3.178	3.178	12
1 0 6	3.083	3.081	29	1 0 4	2.828	2.829	13
0 0 10	3.008	3.006	18	1 1 0	2.760	2.754	9
1 0 7	2.896	2.895	27	1 1 1	2.720	2.716	4
1 1 1	2.757	2.756	55	0 0 7	2.345	2.346	11
1 0 8	2.710	2.708	14	1 0 6	2.241	2.241	3
0 0 12	2.505	2.505	12	0 0 8	2.052	2.053	14
0 0 14	2.146	2.147	34	2 0 0	1.9508	1.9513	7
0 2 0	1.9563	1.9559	28	2 0 1	1.9366	1.9377	3
1 1 13	1.7741	1.7743	22	1 1 7	1.7865	1.7861	5
2 1 6	1.6537	1.6538	13	2 1 3	1.6618	1.6617	4
1 2 7	1.6192	1.6194	17	1 1 8	1.6464	1.6460	5
2 1 8	1.5878	1.5878	8	2 1 4	1.6054	1.6052	5
0 2 14	1.4450	1.4449	16	1 2 4	1.6017	1.6021	4

Intercalation reactions of protonation compound. The protonation compound acts as a solid acid having Brψnsted acid sites similar to those of protonated oxides, such as $HCa_2Nb_3O_{10}$ and $HTiNbO_5$.[4,14] These are capable of incorporating of several organic bases, such as alkylamines and pyridine, between the layers by the acid-base reaction. The protonation compound can also react readily with 1,n-alkyldiamines to form layered alkyldiammonium intercalation compounds. This acid-base reaction produces large increase in the layer separations. The XRD patterns of intercalation compounds are shown in Figure 2 and their lattice parameters are presented in Table 2. As shown in Figure 2, the higher order (00l) reflections could be observed and the (00l) reflections were shifted monotonously to lower 2θ angle with increasing of the alkyl chain length. Although the c parameters increased with the increase of methylene group, the a and b parameters remained constant at 3.91± 0.02 Å. From the unit cell dimensions, the effective interlayer area per alkyl in interlayer compound is 15.3 $Å^2$ for the stoichiometric composition. The linear all-trans hydrocarbon in alkyl chains have cross-sectional area of 18.2 $Å^2$. Therefore, the internal surface area of protonation compound is too small to accommodate close-packed alkyl chains at van der Waals contacts. Consequently, a bilayer structure is expected in primary alk-

Table 2. The lattice parameters and elementary analyses of intercalation compounds

Compound	Lattice constant (Å)			Chemical analysis (wt%)					
	a	b	c	C		H.		N	
				obs.	cal.	obs.	cal.	obs.	cal.
$KSr_2Nb_3O_{10}$	3.920	3.907	30.057						
$HSr_2Nb_3O_{10}\cdot 0.5H_2O$	3.903	3.888	16.424						
$[NH_3(CH_2)_2NH_3]_{0.49}Sr_2Nb_3O_{10}$	3.932	3.911	17.667	1.90	1.87	0.79	0.78	2.03	2.18
$[NH_3(CH_2)_2NH_3]_{0.50}Sr_2Nb_3O_{10}$	3.919	3.906	20.321	3.64	3.65	1.16	1.07	2.08	2.13
$[NH_3(CH_2)_2NH_3]_{0.52}Sr_2Nb_3O_{10}$	3.908	3.894	22.405	5.60	5.33	1.48	1.34	2.08	2.07
$[NH_3(CH_2)_2NH_3]_{0.52}Sr_2Nb_3O_{10}$	3.918	3.906	24.161	7.28	6.96	1.72	1.61	2.08	2.03
$[NH_3(CH_2)_2NH_3]_{0.53}Sr_2Nb_3O_{10}$	3.927	3.904	26.240	8.85	8.51	2.06	1.86	2.09	1.98
$[NH_3(CH_2)_2NH_3]_{0.52}Sr_2Nb_3O_{10}$	3.922	3.907	28.454	10.24	10.03	2.31	2.10	2.00	1.95

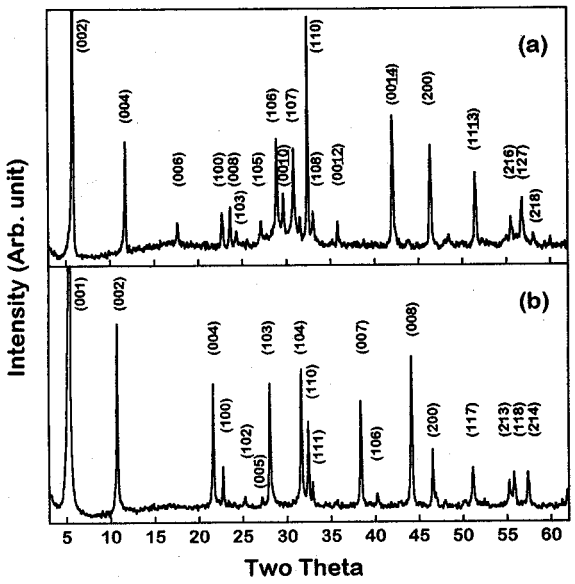

Figure 1. The powder XRD patterns of (a) $KSr_2Nb_3O_{10}$ and (b) $HSr_2Nb_3O_{10}\cdot 0.5H_2O$.

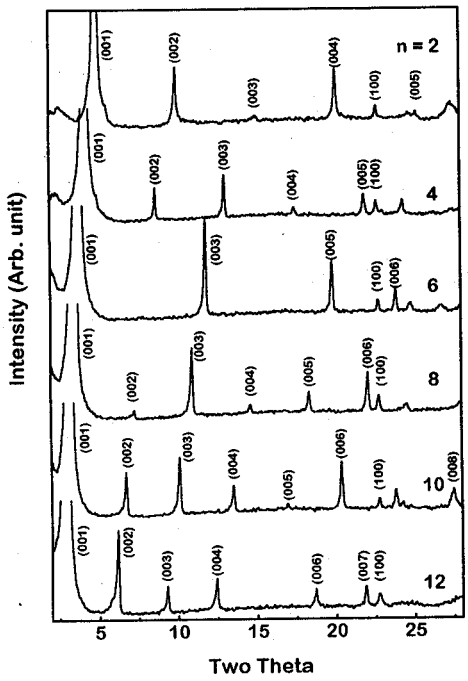

Figure 2. The powder XRD patterns of the intercalation compounds, $[NH_3(CH_2)_nNH_3]_{x/2}Sr_2Nb_3O_{10}$.

ylamines intercalation compounds. However, since the guest molecules are bifunctional diamine molecules, it was observed that the intercalation compounds were made in the forms of monolayer arrangement.

The basal spacings of the intercalation compounds were plotted against the number of carbons in alkyl chain as presented in Figure 3. The interlayer distance increases linearly with the number of carbon atoms in the alkyl chain. The difference in the interlayer distance for each added carbon atom can be estimated from the slope of the curve. A least-square fitting of the data gave $c=1.05n+15.9$ Å where c

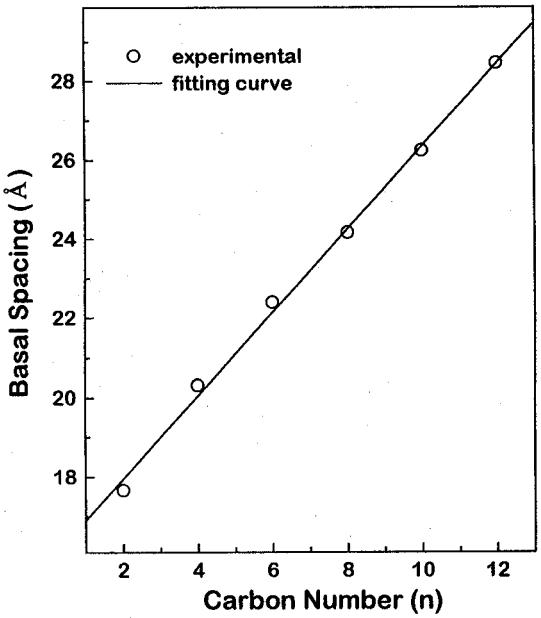

Figure 3. The basal spacing versus carbon number in alkyl chain for theintercalation compounds.

is the c axis spacing and n is the number of carbon atoms in the organic diamine. Assuming the alkyl chains would have all trans-conformations, the chain length grows by 1.27 Å per added alkyl chain. The inclination angle of the alkyl chain with respect to the basal plane is 55.7°, calculated as $\sin^{-1}$ (1.05/1.27). According to Jacobson *et al.*,[15] the primary alkylamine intercalation compounds of $HCa_2Nb_3O_{10}$ are divided into four distinct groups depending on the c-axis expansion. It was reported that the relative strength between van der Waals interaction of the alkyl chains and hydrogen bonding with the oxygen atoms of the layer surface is critical for the relative orientation of the alkyl chain. In our experiments, the inclination angle was similar to the group II in the $HCa_2Nb_3O_{10}$ system. This result implies that, for the diamines intercalation compounds, the hydrogen bonding between the ammonium head group and the oxygen atoms of layer surface controls the chain orientation due to the strong interaction with bifunctional amine groups. In addition to the reaction with alkyldiamine, protonation compound forms intercalation compound with the much weaker base pyridine ($pK_a=5.3$), implying that the protonation compound is nearly as acidic as $HCa_2Nb_3O_{10}$.

The spatial arrangement of alkyldiammonium molecules within the interlayer space can be deduced from the XRD data using one-dimensional electron density projections based on the Fourier summation of the structural factors of the (00l) reflections. The possible orientations and packing of 1,n-alkyldiammonium molecules in the interlayer space and the resulting one dimensional Fourier synthesis are shown in Figure 4. As can be seen in Figure 4, the calculated electron densities are relatively well consistent with the observed one. From this, it can be concluded that the organic diamine molecules are packed to the monolayer oriented to the layer with a tilting angle of *ca.* 56°.

It was confirmed by FT-IR spectra that the intercalation reaction was occurred by the formation of alkyldiammonium

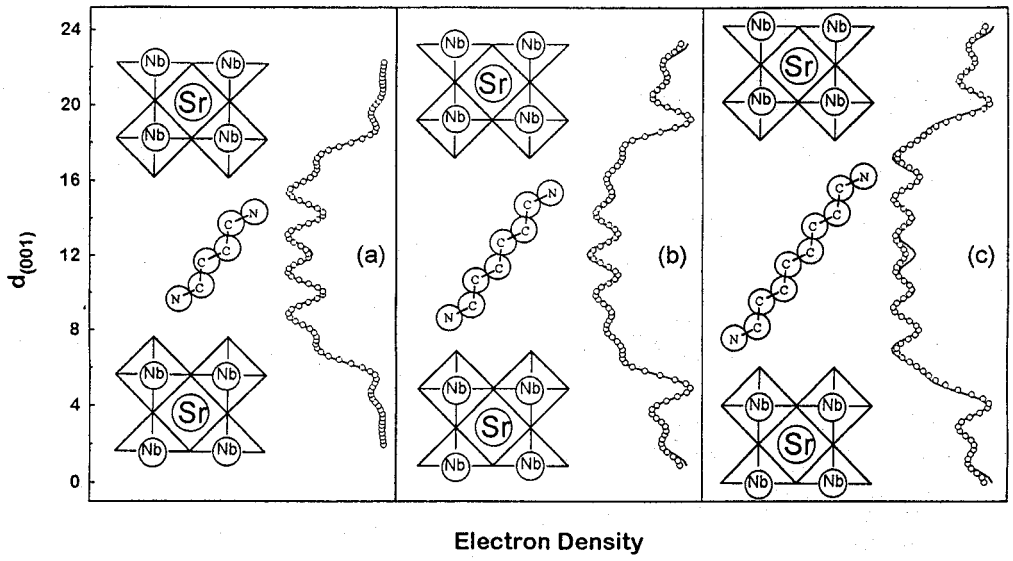

Figure 4. The one-dimensional Fourier synthesis maps and its schematic structures for $[NH_3(CH_2)_nNH_3]_{x/2}Sr_2Nb_3O_{10}$. (a) n=4, (b) n=6, and (c) n=8. (○: experimental, −: calculated)

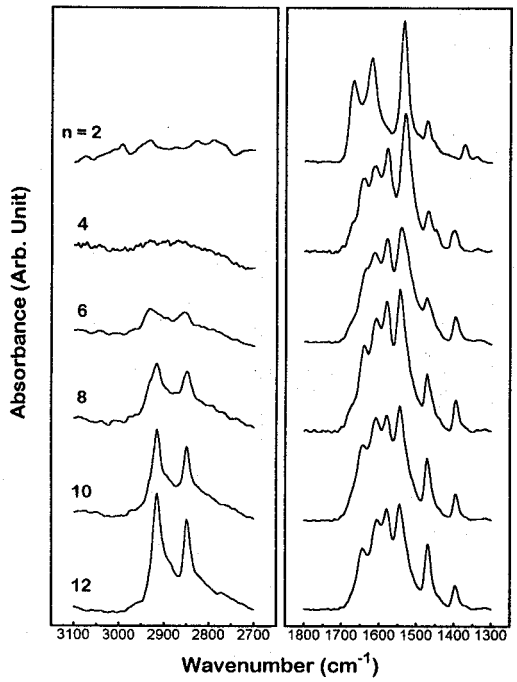

Figure 5. FT-IR spectra of $[NH_3(CH_2)_nNH_3]_{x/2}Sr_2Nb_3O_{10}$.

complexes (Figure 5). The transmittance bands due to $(Sr_2Nb_3O_{10})^{-1}$ layer are seen at 914, 740 and 580 cm^{-1} in the all layered compounds. A pair of strong band in 2911, 2845, and 1470 cm^{-1} at each spectrum can be assigned to the asymmetric, symmetric CH_2 stretching, and CH_2 bending vibration modes, respectively. These peak intensities increase as the number of methylene groups. As the 1,n-alkyldiamines incorporated into the layer, the multicomponent peaks due to bending mode of ammonium group also appeared at 1650-1500 cm^{-1}.

The contents of the intercalated organic diamines were determined by EA (Table 2) under ambient atmosphere. It was confirmed from the C, H, and N analysis of these intercalation compounds that the intercalation reactions occurred stoichiometrically. Whatever the nature of the alkyldiamine may be, the same amount of alkyl diamines, *i.e.*, half a mole per mole of protonation compound were intercalated. This is in good agreement with the complete neutralization of the protonic function of $HSr_2Nb_3O_{10}$ according to the following reaction.

$$HSr_2Nb_3O_{10}+0.5NH_2(CH_2)_nNH_2\rightarrow[NH_3(CH_2)_nNH_3]_{0.5}Sr_2Nb_3O_{10}$$

A series of SEM photographs of the $ASr_2Nb_3O_{10}$ (A=K, H, and 1, n-alkyldiammonium ions) are shown in Figure 6. Apparently, the platelet-like shape of crystals retained during the protonation and intercalation reactions. These results clearly indicate that the reactions occur topotactically. The crystallite sizes of the layered compounds were 1-10 μm and decreased during the protonation and intercalation reactions. In practice, ion exchange often causes fragmentation of solids due to lattice parameter changes; such fragmentation accelerates ion exchange.[16]

Thermal Stability of Intercalation Compounds. The water content was determined by thermogravimetric analysis. The interlayer water is lost below 100 ℃ in a single step. Further heating to 350 ℃ results in a weight loss that corresponds to the loss of the interlayer protons as water. These losses correspond to the loss of interlayer water molecule and interlayer protons forming oxygen defective perovskite structure[7,17] according to the following reaction.

$$HSr_2Nb_3O_{10}\cdot 0.5H_2O\rightarrow HSr_2Nb_3O_{10}\rightarrow Sr_2Nb_3O_{9.5}+1/2H_2O$$

The formation of oxygen deficient phase accompanied with such dehydration was observed often for oxides containing Nb, Ta, and W. Therefore, the composition of protonated compound can be formulated as $HSr_2Nb_3O_{10}\cdot 0.5H_2O$.

The thermal stability of the intercalation compounds were examined by TGA (Figure 7) in air. The weight loss of the intercalation compounds showed distinct three steps. The fraction of the weight loss were 1.5-2.5, 4.4-11.5, and 0.5-4.3% in the temperature ranges 50-120 ℃, 220-500 ℃, and above

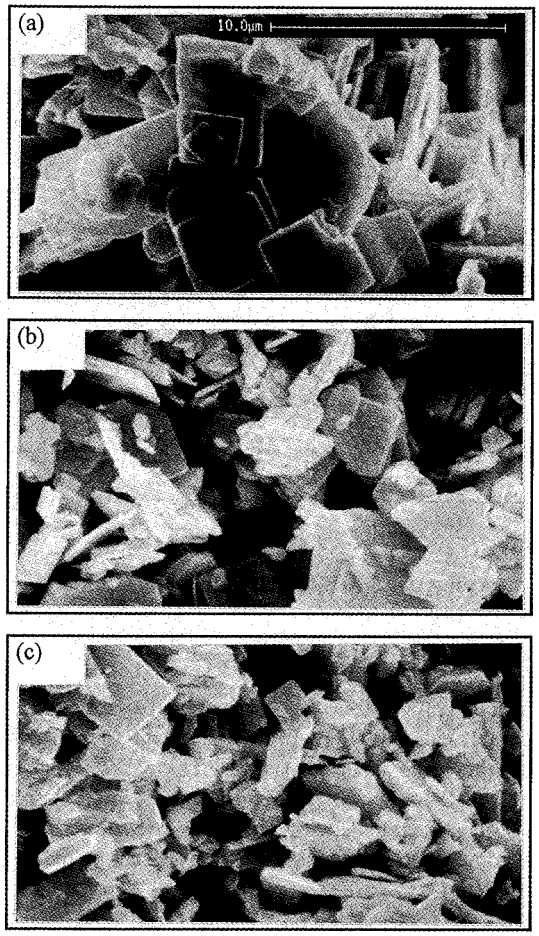

Figure 6. SEM photographs of (a) $KSr_2Nb_3O_{10}$, (b) $HSr_2Nb_3O_{10}\cdot 0.5H_2O$, and (c) $[NH_3(CH_2)_8NH_3]_{0.52}Sr_2Nb_3O_{10}$.

500 ℃, respectively. The weight losses in the first and the second stages correspond to the desorption of hydrated water molecules and the decomposition of organic amines, respectively. The slight weight gain in the temperature ranges 450-630 ℃ may be considered to be the formation of strontium-related compound due to O_2 uptake in the air. Thus, the final weight loss is regarded as the sum of the decomposition of Sr-related compounds and carbon residues. However, we can not certainly figure out why that happens.

The decomposition process of 1,8-octyldiamine intercalation compounds was examined using XRD and IR techniques. The structural changes after heat treatment are shown in Figure 8(a). The basal spacings slowly decreased as increasing of heat treatment temperature. The XRD patterns of the octyldiamine intercalation compound calcined at different temperatures show only shrinkage of the interlayer distance from 24.5 Å to 21.2 Å after heating at 350 ℃. The IR transmittance peaks (Figure 8(b)) at 1470, 2845, and 2911 cm^{-1} (corresponding to C-H bending and C-H symmetric and asymmetric stretching vibration modes, respectively) retained. This might be considered that the shapes of alkyl chain residues retain up to 350 ℃. Further heat treatment up to 500 ℃, the characteristic (001) XRD peak and organic absorption peaks of intercalation compound disappeared, whereas external peak present at 1370-1470 cm^{-1}. This peak may be originated from strontium-related compound, formed as reaction intermediates during the thermal decomposition process. It can be concluded that the 1,8-octyldiamine intercalation compound are thermally stable up to 350 ℃ as observed in other layered titanates.[14] In summary, we have successfully synthesized the layered perovskite oxide $KSr_2Nb_3O_{10}$ and carried out its protonation reaction. This protonation compound, HSr_2-

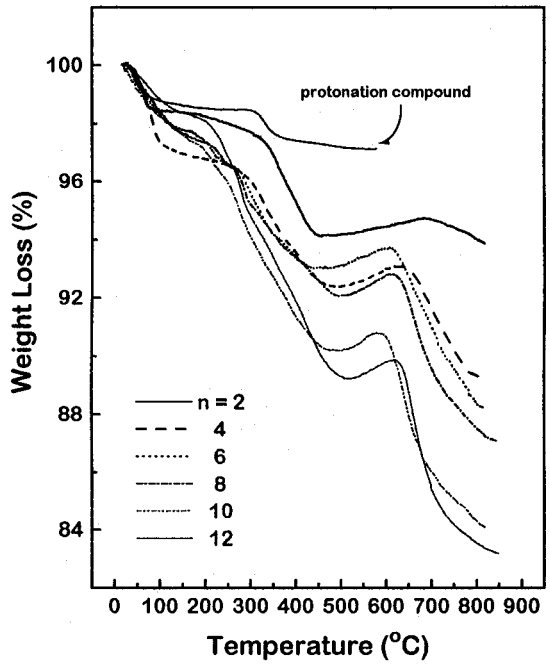

Figure 7. TG curves of protonation compound and $[NH_3(CH_2)_n$-$NH_3]_xSr_2Nb_3O_{10}$.

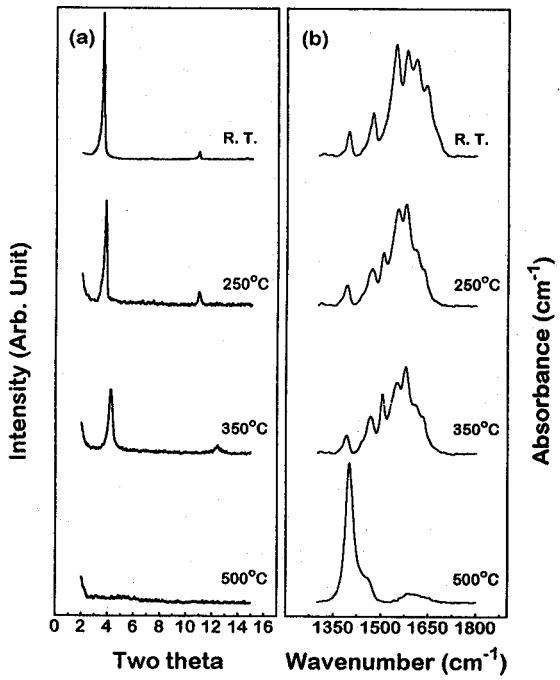

Figure 8. (a) powder XRD patterns and (b) FT-IR spectra for $[NH_3(CH_2)_8NH_3]_{0.52}Sr_2Nb_3O_{10}$ calcined at different temperatures.

$Nb_3O_{10}\cdot 0.5H_2O$, acts as solid acid and reacts with organic bases such as 1,n-alkyldiamines to give intercalation compounds. These intercalation reactions are relatively facile even though the strontium niobate layers are thick and rigid compared to the layers of clay minerals or other oxides known to undergo intercalation reaction. However, the main shortcoming of these organic intercalation compounds for application as catalysts in high temperature is their insufficient thermal stability. We are now investigating the pillaring chemistry of these Dion series oxides using Keggin's ion, $[Al_{13}O_4(OH)_{24}(H_2O)_{12}]^{7+}$.

References

1. Lal, M.; Howe, A. T. *J. Sol. State Chem.* **1984**, *51*, 355.
2. Lichard, M.; Brohan, L.; Tournoux, M. *J. Sol. State Chem.* **1994**, *112*, 345.
3. Wells, A. F. *Structural Inorganic Chemistry*; Clarendon Press: Oxford; 1984 p 602.
4. Dion, M.; Ganne, M.; Tournoux, M. *Mat. Res. Bull.* **1981**, *16*, 1429.
5. Jacobson, A. J.; Johnson, J. W.; Lewandowski, J. T. *Inorg. Chem.* **1985**, *24*, 3727.
6. Gopalakrishnan, J.; Bhat, V. *Mat. Res. Bull.* **1987**, *22*, 413.
7. Gopalakrishnan, J.; Bhat, V. *Inorg. Chem.* **1987**, *26*, 4299.
8. Subramanian, M. A.; Gopalakrishnan, J.; Sleight, A. W. *Mat. Res. Bull.* **1988**, *23*, 837.
9. Thomas, J. M. *J. Chem. Comm. Daton Trans* **1991**, 555.
10. Yoshimura, J.; Ebina, Y.; Kondo, J.; Domen, K.; Tanaka, A. *J. Phys. Chem.* **1993**, *97*, 1970.
11. Anderson, M. W.; Klinowski, J. *Inorg. Chem.* **1990**, *29*, 3260.
12. Tang, X.; Xu, W. Q.; Shen, Y. F.; Suib, S. L. *Chem. Mater.* **1995**, *7*, 102.
13. Jacobson, A. J.; Lewandowski, J. T.; Johnson, J. W. *J. Less-Common Met.* **1986**, *156*, 137.
14. Cheng, S.; Wang, T. C. *Inorg. Chem.* **1989**, *28*, 1283.
15. Jacobson, A. J.; Johnson, J. W.; Lewandowski, J. T. *Mat. Res. Bull.* **1987**, *22*, 45.
16. England, W. A.; Goodenough, J. B.; Wiseman, P. J. *J. Solid State Chem.* **1983**, *49*, 289.
17. Kumada, N.; Takeshita, M.; Muto, F.; Kinomura, N. *Mat. Res. Bull.* **1988**, *23*, 1050.

Molecular Dynamics Simulation of Liquid Alkanes. I. Thermodynamics and Structures of Normal Alkanes: *n*-butane to *n*-heptadecane

Song Hi Lee*, Hong Lee, Hyungsuk Pak†, and Jayendran C. Rasaiah‡

Department of Chemistry, Kyungsung University, Pusan 608-736, Korea
†Department of Chemistry, Seoul National University, Seoul 151-740, Korea
‡Department of Chemistry, University of Maine, Orono, Maine 04469, USA

Received April 29, 1996

We present results of molecular dynamic (MD) simulations for the thermodynamic and structural properties of liquid *n*-alkanes, from *n*-butane to *n*-heptadecane, using three different models I-III. Two of the three classes of models are collapsed atomic models while the third class is an atomistically detailed model. Model I is the original Ryckaert and Bellemans' collapsed atomic model [*Discuss. Faraday Soc.* **1978**, *66*, 95] and model II is the expanded collapsed model which includes C-C bond stretching and C-C-C bond angle bending potentials in addition to Lennard-Jones and torsional potentials of model I. In model III all the carbon and hydrogen atoms in the monomeric units are represented explicitly for the alkane molecules. Excellent agreement of the results of our MD simulations of model I for *n*-butane with those of Edberg *et al.* [*J. Chem. Phys.* **1986**, *84*, 6933], who used a different algorithm confirms the validity of our algorithms for MD simulations of model II for 14 liquid *n*-alkanes and of models I and III for liquid *n*-butane, *n*-decane, and *n*-heptadecane. The thermodynamic and structural properties of models I and II are very similar to each other and the thermodynamic properties of model III for the three *n*-alkanes are not much different from those of models I and II. However, the structural properties of model III are very different from those of models I and II as observed by comparing the radial distribution functions, the average end-to-end distances and the root-mean-squared radii of gyrations.

Introduction

Liquid alkanes exhibit a vast variety of interesting physical properties which follow a pattern starting with methane that is consistent with the alkane structure.[1] An alkane molecule is held together entirely by covalent bonds, which either join two atoms of the same kind and hence are non-polar, or they join two atoms that differ a little in electronegativity